IMAGING 2D RUGGED TOPOGRAPHY SEISMIC DATA: A TOPOGRAPHY PSTM APPROACH INTEGRATED WITH RESIDUAL STATIC CORRECTION

HAO ZHANG, JINCHENG XU, QIANCHENG LIU and JIANFENG ZHANG

Chinese Academy of Sciences, Key Laboratory of Petroleum Resources Research, Institute of Geology and Geophysics, P.O. Box 9825, Beijing 100029, P.R. China. zhanghao@mail.iggcas.ac.cn

(Received January 3, 2016; revised version accepted May 28, 2016)

ABSTRACT

Zhang, H., Xu, J., Liu, Q. and Zhang, J., 2016. Imaging 2D rugged topography seismic data: A topography PSTM approach integrated with residual static correction. *Journal of Seismic Exploration*, 25: 339-358.

Near surface topography is a main challenge in land seismic data processing. In conventional land data processing, seismic data are corrected to a reference datum before migration. We have developed a 2D topography pre-stack time migration (TPSTM) scheme that can handle surface topography with high near-surface velocities in land seismic imaging. The proposed TPSTM can be applied to 2D seismic data recorded on irregular surface without conventional static corrections. We describe the wave propagation through inhomogeneous media by defining two effective velocity parameters with the introduction of a floating datum. As a consequence, wave propagation phenomena in the complex near surface, such as near vertical incidences through a weathering layer and ray paths bending away from vertical in the presence of high near surface velocities, are correctly considered. The two effective velocity parameters can be estimated by velocity analysis and velocity scan so as to flatten events in the imaging gathers. The TPSTM to some extent correctly solves field static correction without applying conventional static correction based on the vertical incidence hypothesis. Applying TPSTM iteratively can also help to update the two velocities defined here and understand the variation of near surface macro velocity. In addition, we integrate residual static corrections into TPSTM to further address the residual static issue. The coherency along the events has been improved for stacking. Two-dimensional field datasets are used to demonstrate the proposed 2D TPSTM and workflow. High-quality imaging results are obtained.

KEY WORDS: land seismic imaging, near surface velocity, topography PSTM (TPSTM), residual static correction.

0963-0651/16/$5.00

INTRODUCTION

Static is one of the most challenging issues in land seismic data processing and imaging. Conventionally, seismic data are corrected to a flat or floating reference datum by static corrections before migration (Yilmaz, 2001). Static corrections are based on the assumption that vertical downgoing and upgoing ray paths through the near-surface layer, applying an entire (static) time shift on each seismic trace (Cox, 1999). However, this assumption failed in the presence of high near-surface velocities. Shtivelman and Canning (1988) analyzed the imaging errors incurred when applying conventional static time shifts. Thus, several wave-equation datuming approaches have been proposed as alternatives to address the complex near-surface issue.

Wave-equation datuming scheme is an effective way for handling rugged topography and several methods have been developed. Berryhill (1979, 1984) and Shtivelman and Canning (1988) propose a scheme based on Kirchhoff-integral-solution. Beasley and Lynn (1992) develop a scheme to correct for the errors caused by static corrections using a conventional finite-difference migration algorithm with a zero layer for migration in the medium between the acquisition surface and the flat datum above the acquisition surface. Bevc (1997) employs a Kirchhoff integral solution propagate the wavefield upwardly to a flat datum above the highest point of the acquisition surface, thus reducing the dependence on the near-surface velocity model in the datuming step. Zhu et al. (1998) use finite-difference-migration-based datuming to field data recorded on rough topography. Alkhalifah and Bagaini (2006) introduce a topographic datuming operator to fill the gap between simple static corrections and more rigorous wave-equation datuming. Al-Ali and Verschuur (2006) implement wave-equation datuming using focusing operators that are determined based on the common-focus-point technique (Berkhout, 1997a, 1997b). It is common for wave-equation datuming to employ a two-step process, i.e., once to continue all common shot gathers and again to continue all common receiver gathers. Liu et al. (2011) propose a doublesquare-root-operator based datuming scheme. However, all these wave-equation datuming based methods have an issue that the number of seismic traces is greatly magnified, thus adding computations for the subsequent processing steps.

Another problem to image the data with topography is the estimation of the near-surface velocity model and the velocity model below the datum. The refraction method and refraction tomography (Zhu et al., 2000; Chang et al., 2002) have been developed to estimate the near-surface velocity model. First breaks or first arrivals need to be picked when one implements the mentioned techniques. However, the lower signal-to-noise ratio caused by rugged topography degrades accuracy in first arrival picking. Many efforts have been made to estimate the interval velocity model below the datum since industry's acceptance of prestack depth migration (PSDM) (Kabir and Verschuur, 2000;

Biondi and Symes, 2004; Virieux and Operto, 2009). However, the velocity model estimation remains a challenging task for pre-stack depth migration (PSDM).

Prestack time migration (PSTM) has proven to be efficient in imaging complicated reflectors in the absence of strong velocity variations. Although PSTM misposition events in the presence of lateral velocity variations (it is possible to correct the positional errors using a subsequent time-depth conversion), it can give a good indication of faults and interfaces because the reflected energies are well focused. Another attractive characteristic of PSTM is that the migration velocity model can be determined by velocity analysis and velocity scanning.

In this paper, we develop a 2D topography PSTM (TPSTM) scheme to image 2D topography data directly without field static correction. The method we propose introduces a floating datum which is the starting point for imaging and uses two effective velocity parameters, the near surface macro velocity and root-mean-square velocity from datum to imaging point to calculate the traveltime and amplitude. This method partially solves the field static correction during migration process and can invert the macro near surface velocity model and imaging velocity. For the real data in practice, there are still some residual static showing in the CRP gathers after TPSTM. Thus we further develop the residual static estimation based on CRP gathers after migration instead of estimation on CMP gather before migration. For the paper structure, we first present the formulations to compute traveltime and amplitude using two effective velocity parameters for wave propagation through inhomogeneous media above and below the datum, which is the foundation of the imaging algorithm. Further we demonstrate the influence of the two velocity parameters defined. Then we introduce the residual static correction based on the CRP gather after TPSTM. Finally, we demonstrate the method and workflow with a 2D real dataset.

TRAVELTIME AND AMPLITUDE CALCULATION OF 2D TOPOGRAPHY PSTM METHOD

For the land seismic data, it is often acquired on rugged topography surface. Conventionally we introduce a reference datum and apply static correction to vertically shift the data to the datum and employ conventional processing. In this paper, we define two effective velocity parameters and derive the formulations to compute traveltime and amplitude for wave propagation through inhomogeneous media above and below the datum using the phase-shift method (Gazdag, 1978). The illustration of this definition is shown in Fig. 1. Detailed derivations are given in Appendix A. The traveltime (τ) and amplitude (A) of the wave propagating from the receiver or shot to the imaging point are given by

$$\tau = [T_2/\sqrt{(1+\eta^2)}][1 + a_1\sqrt{\{1+(1-a_2^2\eta^2)\}} + \eta a_3] \quad , \tag{1}$$

$$A = [1 + (1-a_2^2)\eta^2]/[T_2 V_{rms}^2(1+\eta^2)] \times \{a_1 a_2^2 + [1 + (1-a_2^2)\eta^2]^{3/2}\}^{-1/2} \times \{a_1 a_2^2 + [1 + (1-a_2^2)\eta^2]^{1/2}\}^{-1/2} \quad , \tag{2}$$

where a_1, a_2 and a_3 are non-dimensional parameters that read

$$a_1 = T_1/T_2, \quad a_2 = V_0/V_{rms}, \quad a_3 = (x - x_g)/T_2 V_{rms}, \tag{3}$$

and η is the positive root of the equation:

$$\{a_1 a_2^2 \eta/\sqrt{[1 + (1-a_2^2)\eta^2]}\} + \eta - a_3 = 0 \quad . \tag{4}$$

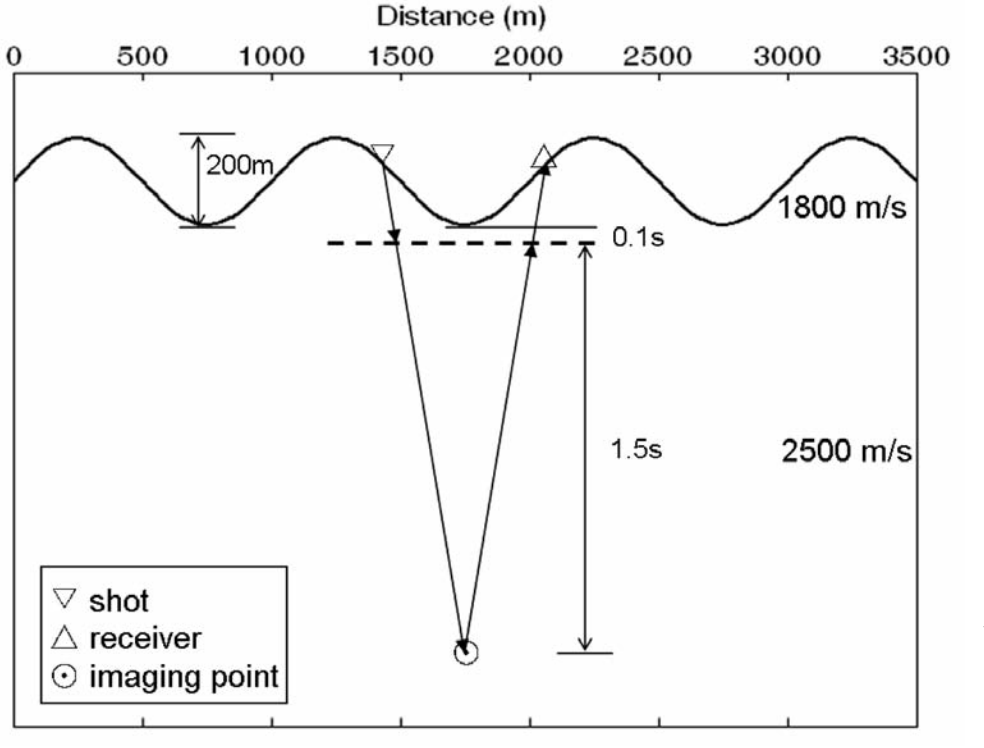

Fig. 1. Model with a sinusoidal acquisition surface used to express the effects of the topography scenario and two velocity parameters. The flat dashed line denotes the datum. The media above and below the datum are homogeneous with velocities of 1800 m/s and 2500 m/s, respectively.

Here, v_0 and v_{rms} are the two effective velocity parameters defined as macro near surface velocity from surface to floating datum and imaging velocity from floating datum to imaging point. T_1 and T_2 are the one-way vertical traveltime from the shot or receiver to the datum level and from datum level to the imaging point level, respectively; x_g and x are the lateral coordinates of the shot or receiver and the imaging point, respectively.

Eqs. (1) and (4) are equivalent to Snell's law for two homogeneous media with the velocities of v_0 and v_{rms} above and below the datum. This validates eqs. (1) and (4). In practice, eqs. (1) and (4) explain how to determine the effective velocities when Snell's law is applied to inhomogeneous media. Moreover, eq. (2) gives the amplitude for wave propagation through inhomogeneous media above and below the datum. Although eqs. (1), (2) and (4) are derived based on the assumption of layered media, they can handle laterally inhomogeneous media by allowing v_{rms} to vary vertically and laterally and v_0 to vary laterally. Eqs. (1), (2) and (4) provide the foundation for the proposed 2D TPSTM.

Since we obtain the traveltime and amplitude weight, applying deconvolution imaging condition (Claerbout, 1971) yields

$$I(x,T_2) = (A_g/A_s) \int F(\omega)\sqrt{\omega}\, \exp[-j(\pi/4)]\, \exp[j\omega(\tau_s+\tau_g)]d\omega \quad , \qquad (5)$$

where $F(\omega)$ is the Fourier transform of the input trace, τ_s, τ_g and A_s, A_g denote the traveltime and amplitude representing the source side and receiver side, respectively.

ESTIMATION OF TWO VELOCITY PARAMETERS

Since the 2D TPSTM scheme are based on eq. (5), the defined two velocity parameters v_0 and v_{rms} are the key parameters needed for this scheme. Using given v_0 and v_{rms}, looping through each seismic trace and accumulating the corresponding imaging result obtained using eq. (5) according to (x,T_2,H), we can obtain the CRP gathers for the predefined, regularly spaced lateral position. Here H is the offset at the datum level. An appropriate migration aperture needs to be imposed in the computation of eq. (5), which is confined to the range of the imaging volume. The resulting CRP gathers expressed in T_2 and H will be the same as those obtained in conventional PSTM. Stacking the CRP gathers along H yields a migration stacked section. Thus flatness of the events in CRP gathers gives indication and criteria for updating the two velocities v_0 and v_{rms}.

The TPSTM allows v_0 vary slowly with the lateral positions of shots and receivers or imaging points. Here in practice the lateral position of v_0 and v_{rms} are corresponding to the lateral position of imaging points. Thus the behaviors of the events in a CRP gather will be determined only by one v_0 at each CDP (imaging) location, and we can estimate v_0 by percentage scanning. Once the correct v_0 is determined, we can continue to flat the events in CRP gathers by velocity analysis with respect to v_{rms}. Thus, we can estimate v_{rms} from CRP gathers following conventional PSTM. Hence, velocity estimation becomes feasible and we can update the two velocities through iterations.

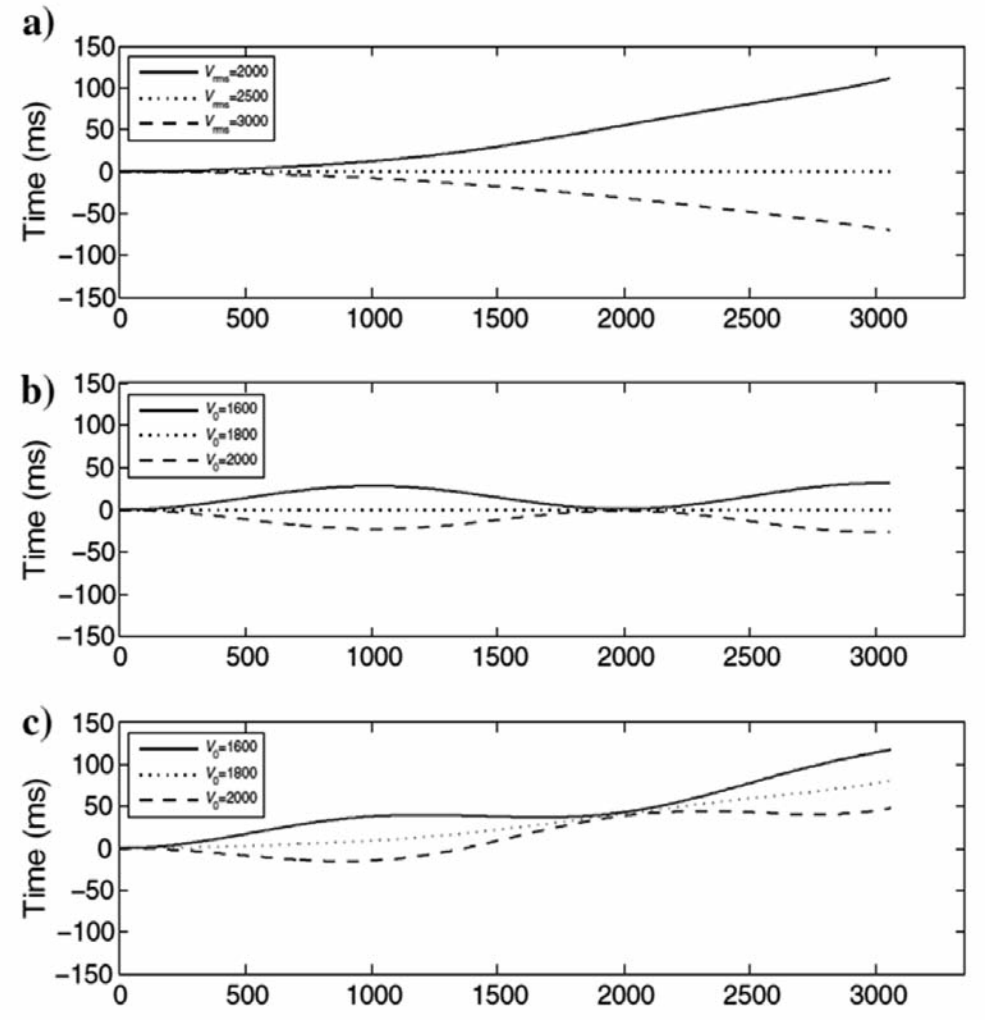

Fig. 2. Residual traveltime curves for an imaging point under a few different combinations of two velocity parameters. Panel (a) is related to a correct v_0 and different v_{rms}; (b) a correct v_{rms} and different v_0; (c) an inaccurate v_{rms} (v_{rms} = 2100 m/s) and the same v_0 as (b).

A numerical analysis with respect to v_0 and v_{rms} is illustrated in Fig. 2 which explains the different contributions of the two velocity parameters. Fig. 2 shows the residual traveltime vary with offsets when a few different combinations of v_0 and v_{rms} are tested. If the v_0 is correct, we show that the residual traveltime vary with offset at datum level. From Fig. 2 we find that an inaccurate v_0 results in short-wavelength divergences of traveltime while the inaccuracy of v_{rms} mainly influents the hyperbolic behavior of the events. This implies that parameter v_{rms} can be updated by minimizing the residual moveout and parameter v_0 can be determined by scanning according to the gather behavior at shallow events. To summarize, the strategy to estimate the two velocity parameters is proposed as follows: (1) Migrate the data using proposed TPSTM with initial v_0 and v_{rms} (2) update v_{rms} by minimizing the residual moveout under given v_0 and (3) scan and pick up v_0 according to flatness of shallow events under updated v_{rms} and (4) finally using both updated v_0 and v_{rms} to re-migrate the data and obtain the final result.

INTEGRATION WITH RESIDUAL STATIC CORRECTION

It is known that the static can be categorized as field static component and residual static component. The former mainly comes from elevation fluctuation of the surface above the datum while the latter comes from improper field static correction or field acquisition measurement error (Cox, 1999). Although the TPSTM scheme compensates field static effect during migration, however, for the real data, the small time distortions, which may originate from the rapid variations in the near-surface velocities or errors in the acquisition, still exist after TPSTM. Conventionally, residual static time shifts are evaluated from common midpoint (CMP) gathers after conventional field static and NMO corrections (Yilmaz, 2001). Due to the fact that some reflectors do not exhibit hyperbolic events in CMP gathers in the presence of complicated structures, the residual static time shifts estimated from CMP gathers will not fully eliminate the small time distortions included in CRP gathers obtained using the pre-stack migration.

Thus, after TPSTM, it is natural to integrate residual static corrections into the migration workflow. Here the new method is to estimate the residual time shift from migrated gathers generated by TPSTM instead of using the pre-migration CMP gathers. However in the CRP gathers generated from TPSTM, the contributions for residual static from different shots and receivers are mixed. To integrate residual static corrections into TPSTM, we need to produce the common imaging gathers expressed in terms of shot and receiver locations.

Specifically, we loop over each seismic trace and stacking the corresponding imaging result obtained using eq. (5) according to shot

coordinates (or receiver coordinates) rather than offset, we can obtain imaging gathers expressed in shot or receiver locations instead of CDP location. Because the residual time shifts are picked in a limited time window (as in conventional residual static corrections), we only need to generate imaging gathers in a prescribed spatially varying time window. Note that this process should be performed after correct v_0 and v_{rms} have been obtained. Moreover, stretch mute and residual NMO should be applied to each migrated trace before the trace is stacked into imaging gathers.

After generating imaging gathers expressed in terms of shot and receiver locations, we can estimate the residual time shifts for each shot and receiver location using the method of Ronen and Claerbout (1985), that is, (1) cross-correlating a super trace built from all traces in an imaging gather and (2) for each lateral position k, we selected the migrated trace from imaging gathers $g_j(T)$ expressed in shot or receiver location. Meanwhile we selected another trace $p_k(T)$ from the stack section as per the same lateral position k. We do a cross-correlation using the formula

$$\phi_{jk}(\tau) = \sum_{T=T_1}^{T_2} g_j(T)[p_k(T+\tau) - g_j(T+\tau)] \Big/ \Big[\sum_{T=T_1}^{T_2} g_j^2(T)\Big]^{1/2}\Big[\sum_{T=T_1}^{T_2}\{p_k(T) - g_j(T)\}^2\Big]^{1/2}, \quad |\tau| < \Delta \tag{6}$$

where T_1, T_2 is the limited time window range for calculating the cross-correlation function, Δ is the maximum limitation of the residual static in this location. Then searching the time associated with the global maximum of the cross-correlation result, which is the residual static t_{jk}. To emphasize the peak value of the cross-correlation function, we construct the function

$$W(\tau) = \phi_{jk}(\tau) / [1 - \phi_{jk}^2(\tau)] \ . \tag{7}$$

We pick the peak value in the function $W(\tau)$ instead of $\phi_{jk}(\tau)$ directly. The time obtained for each trace in each imaging gather is the residual time shift related to the shot location (corresponding to the trace) and lateral position (corresponding to the CDP position of the imaging gather). The median value of the time shifts in a group at a common shot location but different lateral positions is exactly the surface-consistent residual time shift of the shot location. Based on the imaging gathers expressed in the receiver locations, we can obtain the surface consistent residual time shift for each receiver location in the same way.

Evaluating the shot and receiver residual time shifts according to the shot and receiver locations, respectively, and incorporating the sum of the shot and receiver residual time shifts to the corresponding trace when migrating under the

correct v_0 and v_{rms} using TPSTM again, we obtain the modified CRP gathers. Muting the stretched parts of long offsets and stacking the CRP gathers along the offset yield a final migration stacked section.

2D FIELD DATA EXAMPLE

We apply our method on a 2D field dataset from northwestern China. In total this dataset consists of 560 shots and each shot contains 240 recording channels. The data recording length is 6 seconds with a sampling rate of 4 ms. The shot interval is 50 meters while the geophones are spaced at 25 m intervals. The offset ranges from 100 to 3200 m. The surface topography can be observed in Fig. 3, where the surface elevation varies from 360 to 540 m, the dashed line here denotes the reference datum. From a typical shot gather displayed in Fig. 4 we note that the events in the shot data are distorted and discontinuities can be observed due to rapid changes of surface elevation.

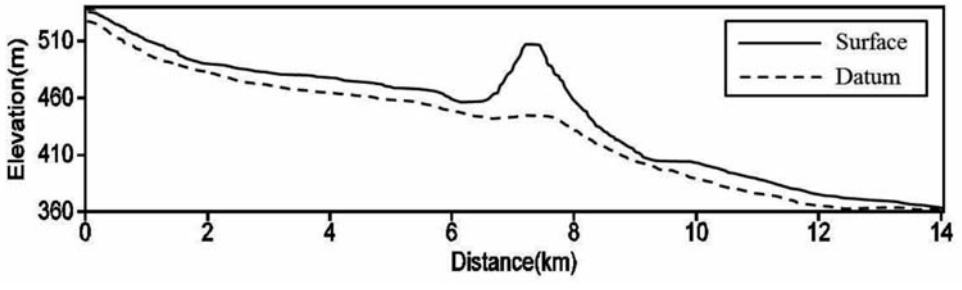

Fig. 3. Surface elevation (solid line)of the 2D field data where the dashed line denotes the floating datum.

The ideal situation is to position the datum at the interface between the low and high velocity media in the near surface. As shown in Fig. 3, we smooth the surface and shift down as the datum. The initial v_0 is assumed to be lateral invariant with a value of 950 m/s. The laterally invariant, initial v_{rms} (Fig. 7a) is obtained by averaging the velocities obtained using conventional NMO at selected lateral positions over the imaging space.

The velocity parameters are updated at regular sampled lateral positions. As shown in Fig. 6, we scan v_0 and migrate the data and produce a gather panel to determine the optimal percentage value to update v_0 at selected locations. The updated, laterally varying v_0 is illustrated with solid line in Fig. 5. Fig. 7b shows the updated inhomogeneous v_{rms}. Once we get the optimal v_0 and v_{rms}, we migrate the data again to produce the image as shown in Fig. 8. Although no field static correction is applied, we obtain continuous events and clear image with our method.

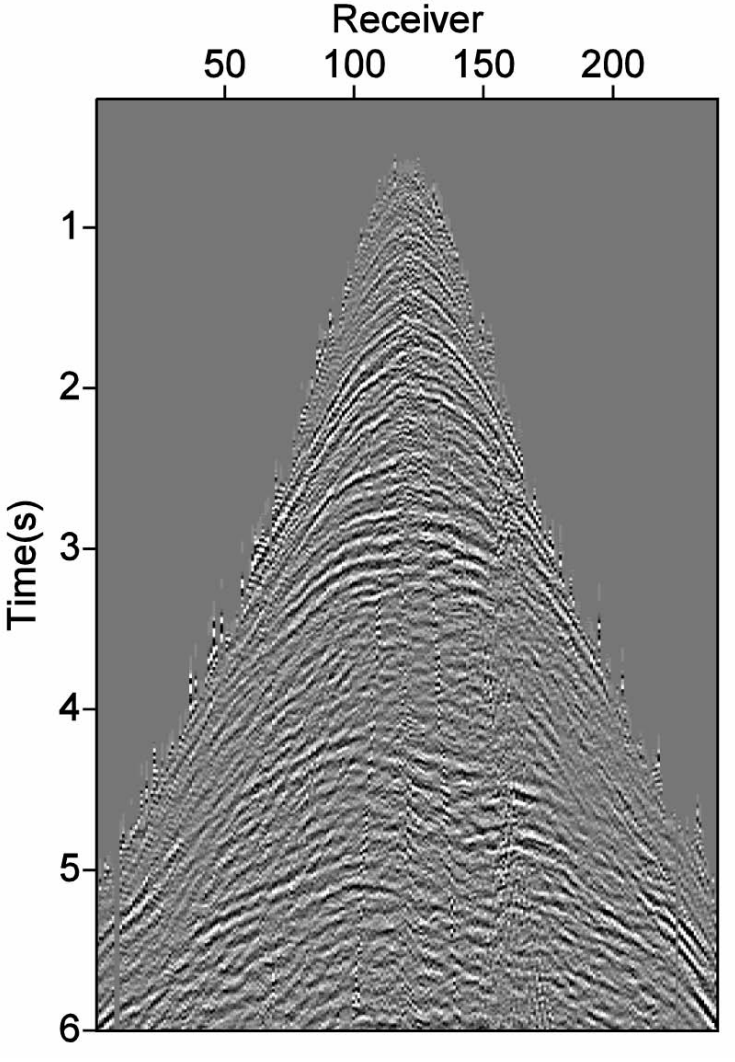

Fig. 4. Typical shot gather of 2D field dataset. The events in the shot data are distorted and discontinuities can be observed due to rapid changes of surface elevation.

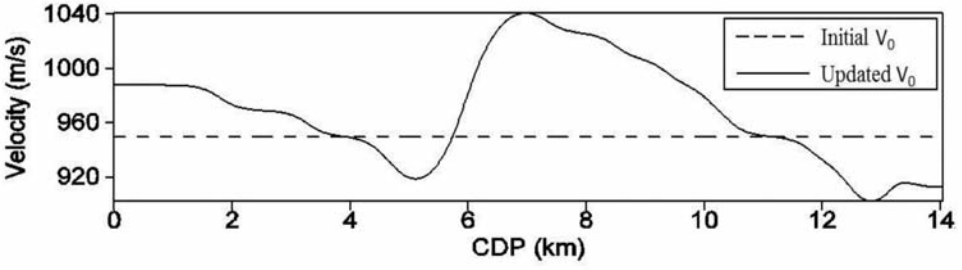

Fig. 5. Comparison of initial and updated near surface macro velocity v_0.

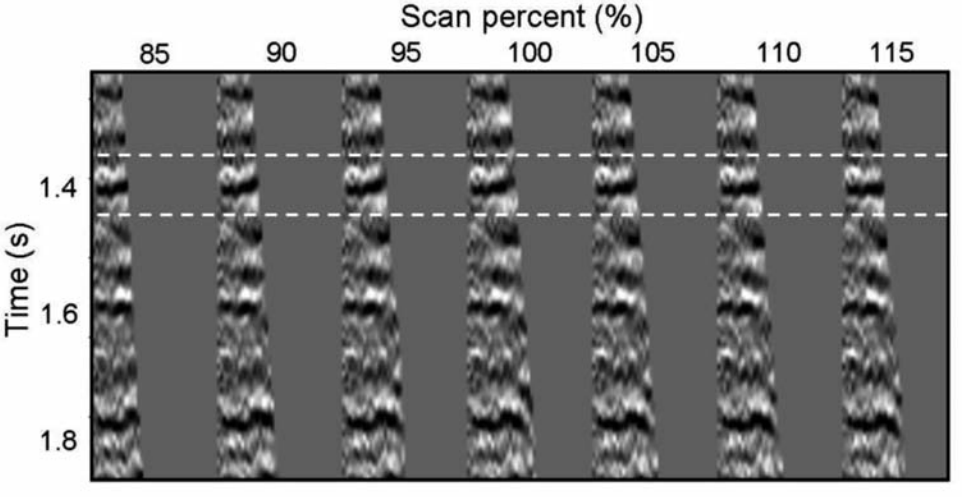

Fig. 6. Modification of v_0 in terms of percentage scanning based on initial v_0 and generating CRP gathers at location CDP 7 km. We note that 110% of initial v_0 gives optimal gather flatness between the time window (white dashed line) at shallow. We use 110% to update initial v_0 at this location.

Further, we use the final v_0 and v_{rms} to produce the imaging gathers in terms of shot location group and receiver location group respectively (Figs. 9b and 9c). We select the trace from them and do cross-correlation using eq. (6) to generate the residual static as per every shot and CDP location. Then we calculate the median value at adjacent CDP location and determine this time shift value as the residual static for this shot group location. For the receiver side, we obtain the residual static for each receiver location group in the same way. Fig. 10 shows the residual static in terms of shot location group and

receiver location group respectively. Then we compensate this residual static in the data and reproduce the CRP gathers as shown in Fig. 11. We note that the small time distortions on gathers have been mitigated and coherency of the event has been improved. Finally we stack the improved CRP gathers to generate the final image as shown in Fig. 12. In order to further evaluate the new approach, we zoom in and compare the imaging result using the new method shown in Fig. 13b with the result generated by conventional static correction based method shown in Fig. 13a. The events are well imaged and the continuity has been improved due to introduction of the residual static correction in the new approach.

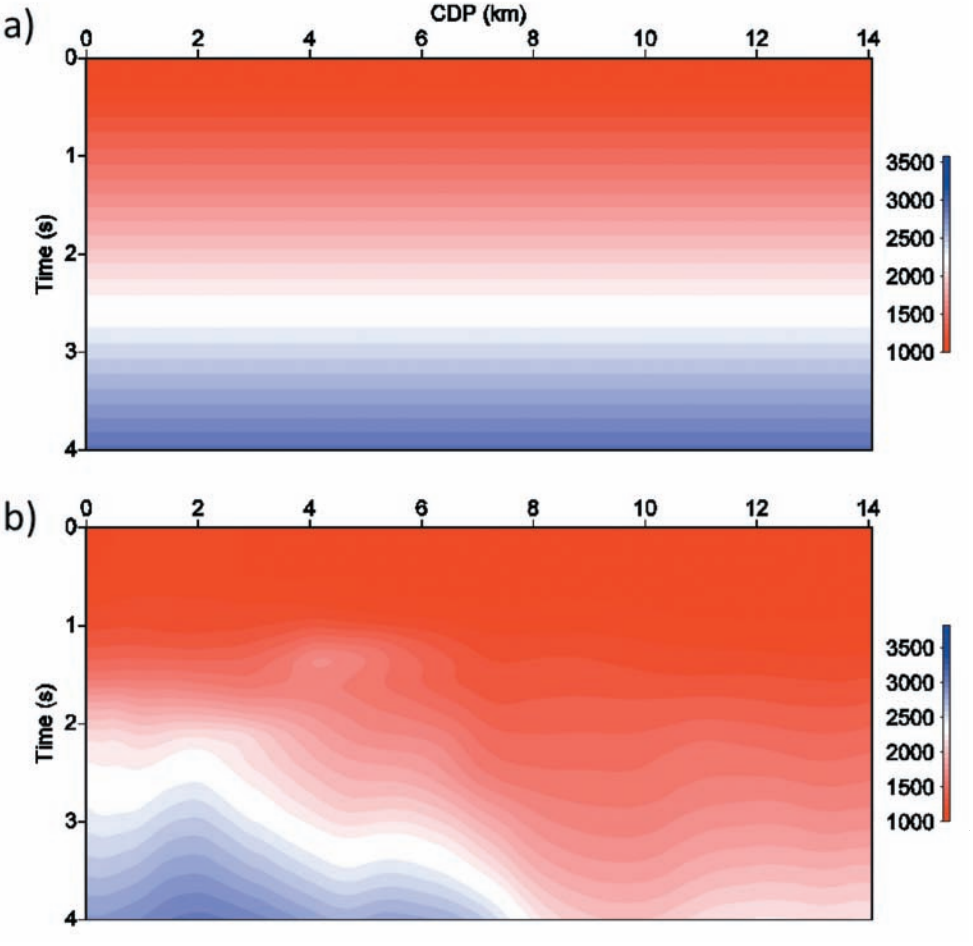

Fig. 7. Comparison of initial and updated imaging velocity v_{rms} below datum. Note that the time is corresponding to T_2.

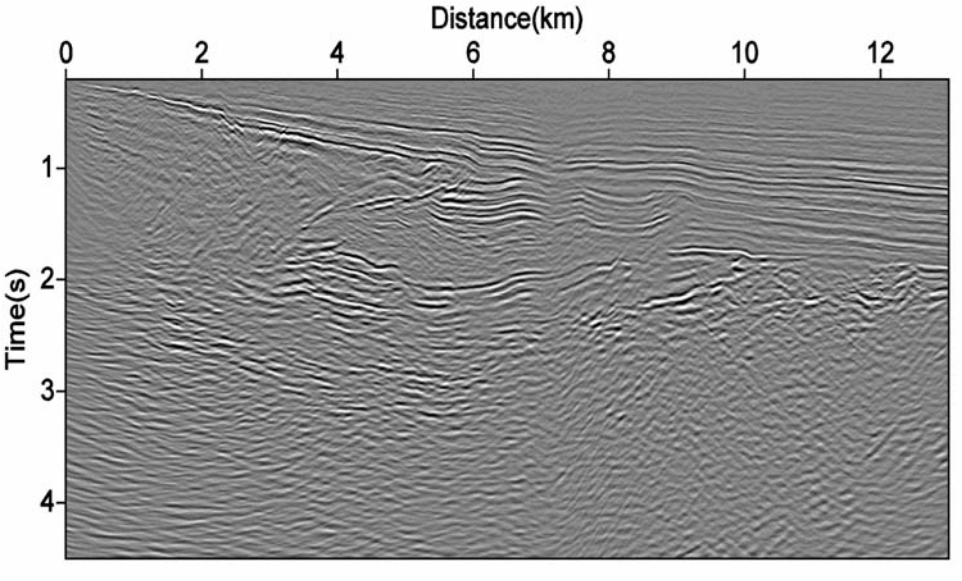

Fig. 8. Imaging result by topography PSTM using updated v_0 and v_{rms}.

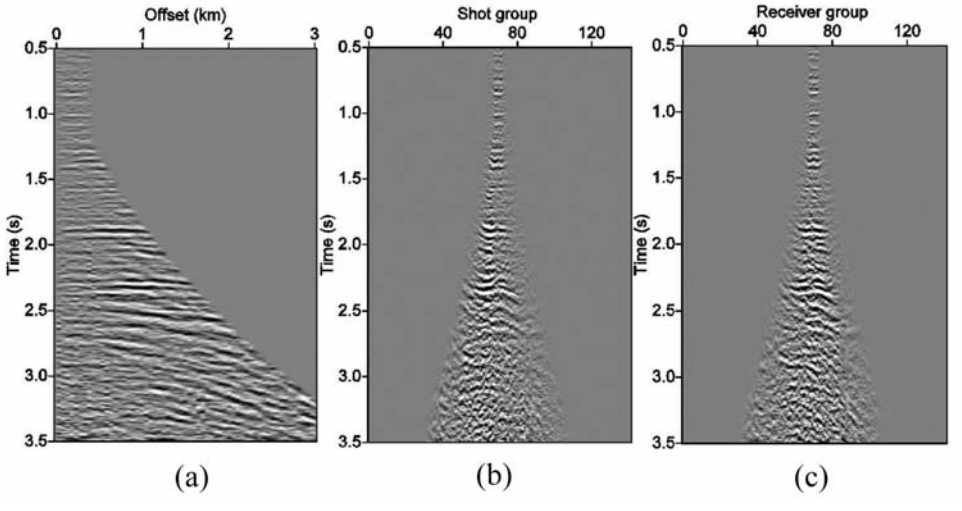

Fig. 9. Topography PSTM CRP gathers expressed by (a) offset (b) shot location group (c) receiver location group.

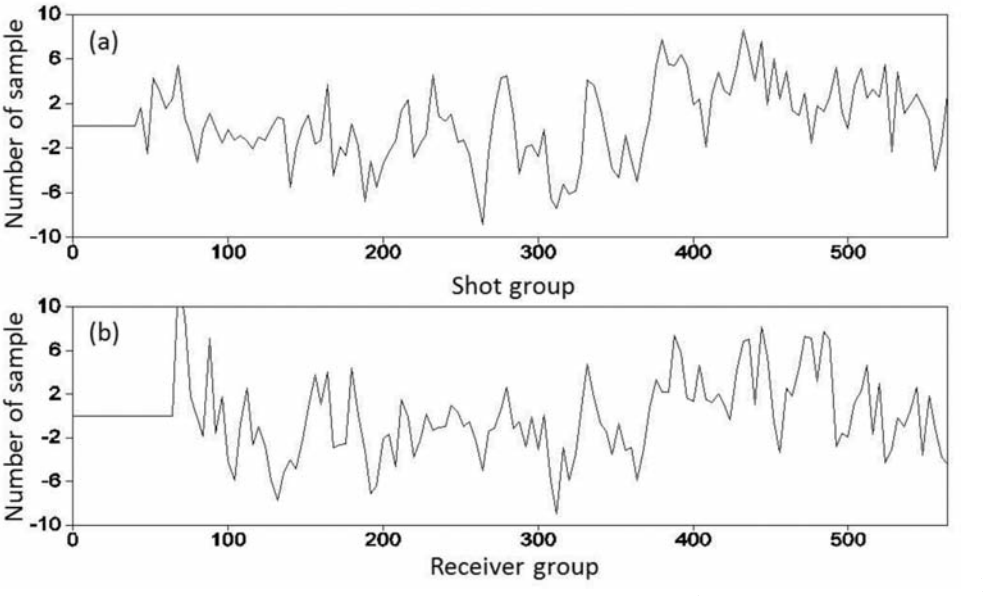

Fig. 10. Residual statics with respect to (a) shot position group and (b) receiver position group.

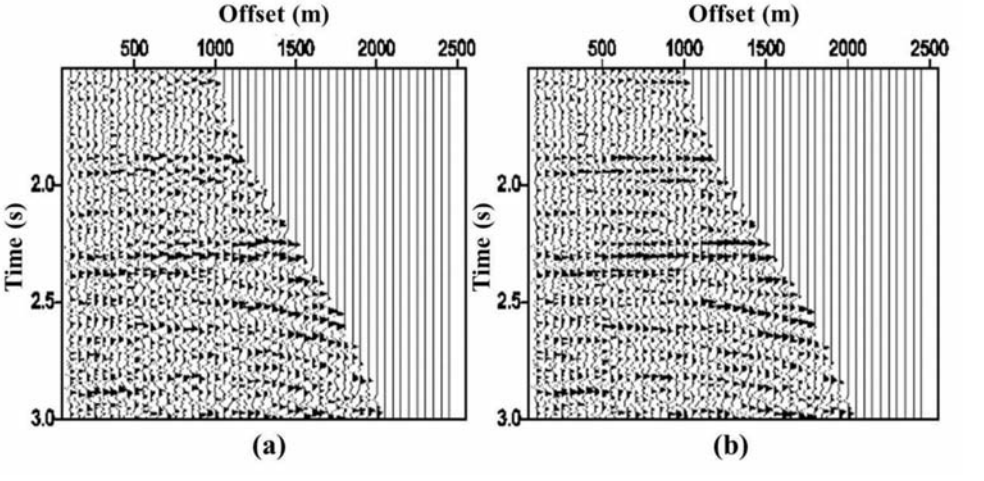

Fig. 11. CRP gathers (a) without residual static correction and (b) with residual static correction.

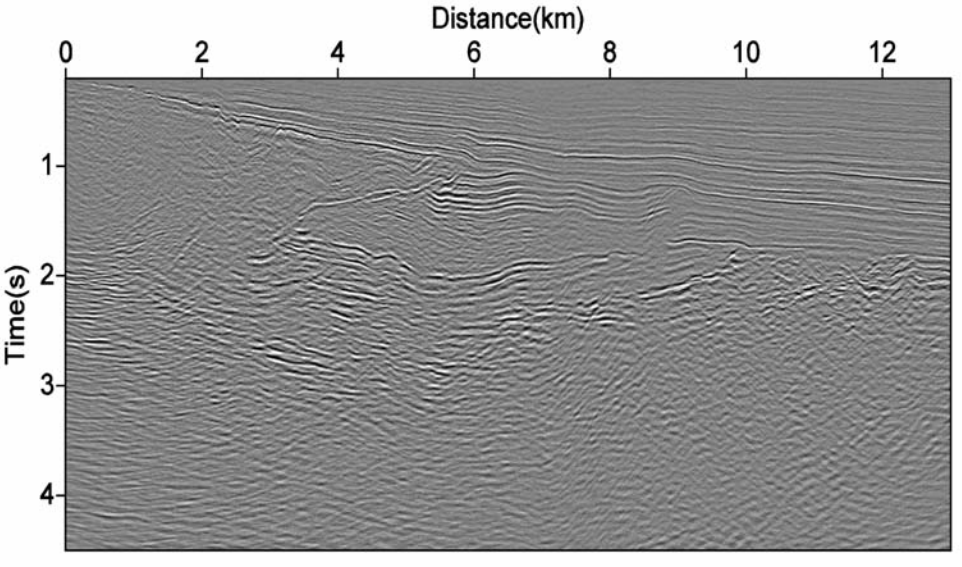

Fig. 12. Final topography imaging result using the data with residual static correction.

CONCLUSIONS

We have presented a 2D topography PSTM scheme that can directly migrate the seismic data recorded on rugged near surface. The TPSTM has extensive uses where the near-surface velocities vary from one extreme of being very low to the extreme of being equivalent to the underlying medium velocity. Moreover, TPSTM allows low and high near-surface velocities to exist simultaneously in the model. Using TPSTM iteratively can update or build the migration velocity fields above and below the datum by flattening events in imaging gathers.

TPSTM can image complicated reflectors and faults only in the absence of strong velocity variations. We also extend TPSTM to include (surface consistent) residual static corrections. Unlike conventional residual static corrections, the residual static time shifts are determined after migration. This improves focusing and continuity of events, as demonstrated by the field data example. TPSTM has been applied to 2D field dataset. Compared with the conventional static correction based method, TPSTM integrated with residual static correction can give high-quality imaging result.

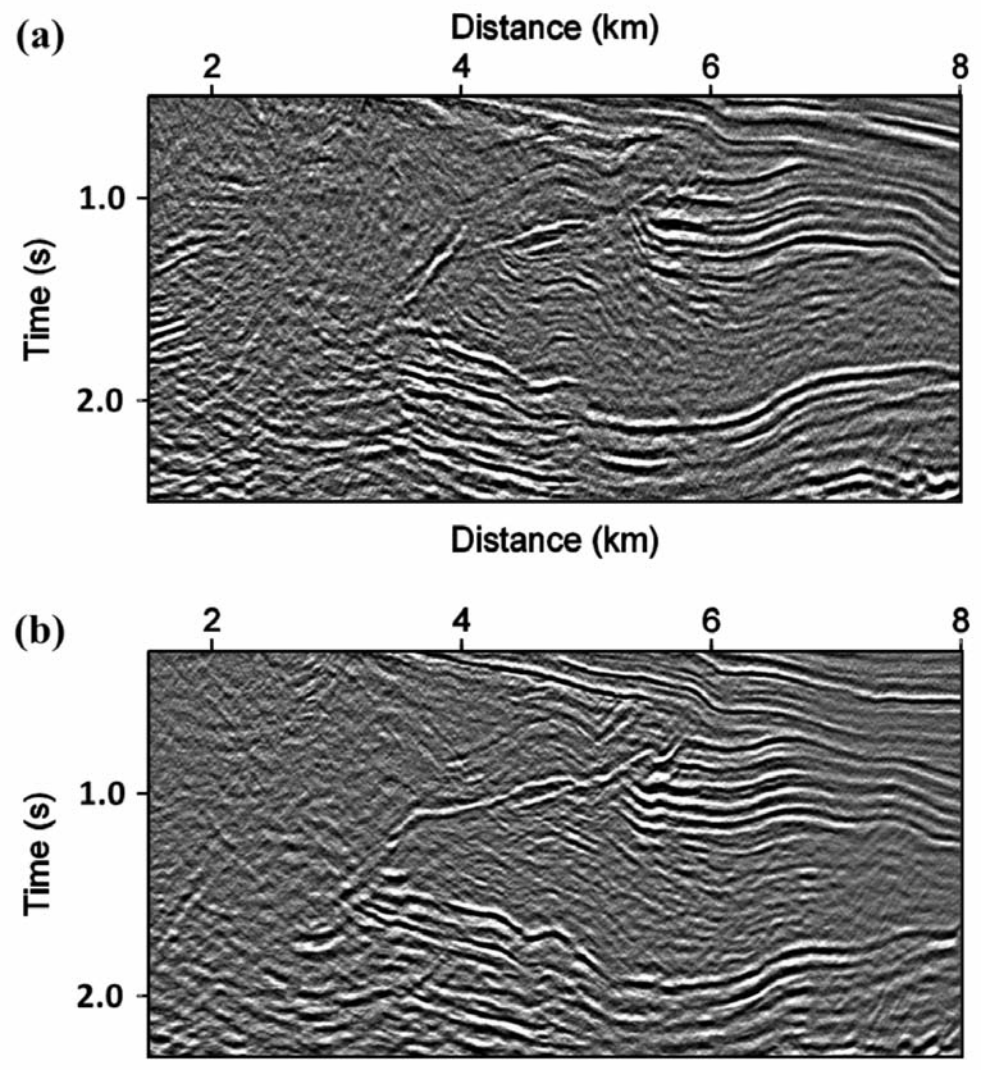

Fig. 13. Imaging result comparison: a) conventional method; b) new method.

ACKNOWLEDGMENTS

The authors are grateful to the National Science Fund of China (under grant No. 41174112) and National Science Fund of China Key Project (under grant No. 41330316) for supporting this work.

We thank PetroChina Northwestern division for providing the 2D dataset. We acknowledge the anonymous reviewers for their valuable comments and suggestions, which greatly improved this manuscript.

REFERENCES

Alkhalifah, T. and Bagaini, C., 2006. Straight-rays redatuming: A fast and robust alternative to wave-equation-based datuming. Geophysics, 71(3): U37-U46. doi: 10.1190/1.2196032.

Al-Ali, M.N. and Verschuur, D.J., 2006. An integrated method for resolving the seismic complex near-surface problem. Geophys. Prosp., 54: 739-750. doi: 10.1111/gpr.2006.54.issue-6.

Beasley, C. and Lynn, W., 1992. The zero-velocity layer: Migration from irregular surfaces. Geophysics, 57: 1435-1443. doi: 10.1190/1.1443211.

Berkhout, A.J., 1997a. Pushing the limits of seismic imaging, Part I: Prestack migration in terms of double dynamic focusing. Geophysics, 62: 937-953. doi: 10.1190/1.1444201.

Berkhout, A.J., 1997b. Pushing the limits of seismic imaging, Part II: Integration of prestack migration, velocity estimation, and AVO analysis. Geophysics, 62: 954-969. doi: 10.1190/1.1444202.

Bevc, D., 1997. Flooding the topography: Wave-equation datuming of land data with rugged acquisition topography. Geophysics, 62: 1558-1569. doi:10.1190/1.1444258.

Biondi, B. and Symes, W.W., 2004. Angle-domain common-image gathers for migration velocity analysis by wavefield-continuation imaging. Geophysics, 69: 1283-1298. doi: 10.1190/1.1801945.

Berryhill, J.R., 1979. Wave-equation datuming. Geophysics, 44: 1329-1344. doi: 10.1190/1.1441010.

Berryhill, J.R., 1984. Wave-equation datuming before stack. Geophysics, 49: 2064-2066. doi: 10.1190/1.1441620.

Bleistein, N., 1984. Mathematical Methods for Wave Phenomena. Academic Press, Inc., New York.

Claerbout, J.F., 1971. Toward a unified theory of reflector mapping. Geophysics, 36: 467-481. doi: 10.1190/1.1440185.

Cox, M., 1999. Static Corrections for Seismic Reflection Surveys. SEG, Tulsa, OK.

Chang, X., Liu, Y., Wang, H., Li, F. and Chen, J., 2002. 3-D tomographic static correction. Geophysics, 67: 1275-1285. doi: 10.1190/1.1500390.

Gazdag, J., 1978. Wave equation migration with the phase-shift method. Geophysics, 43: 1342-1351. doi: 10.1190/1.1440899.

Kabir, M.M.N. and Verschuur, D.J., 2000. A constrained parametric inversion for velocity analysis based on CFP technology. Geophysics, 65: 1210-1222. doi: 10.1190/1.1444813.

Liu, W., Zhao, B., Zhou, H., He, Z., Liu, H. and Du, Z., 2011. Wave-equation global datuming based on the double square root operator. Geophysics, 76(3): U35-U43. doi: 10.1190/1.3555076.

Ronen, J. and Claerbout, J.F., 1985. Surface-consistent residual statics estimation by stack-power maximization. Geophysics, 50: 2759-2767. doi:10.1190/1.1441896.

Shtivelman, V. and Canning, A., 1988. Datum correction by wave equation extrapolation. Geophysics, 53: 1311-1322. doi: 10.1190/1.1442409.

Virieux, J. and Operto, S., 2009. An overview of full-waveform inversion in exploration geophysics. Geophysics, 74(6): WCC1-WCC26. doi: 10.1190/13238367.

Yilmaz, Ö., 2001. Seismic Data Analysis: Processing, Inversion, and Interpretation of Seismic Data. SEG, Tulsa, OK.

Zhu, X., Angstman, B.G. and Sixta, D.P., 1998. Overthrust imaging with tomo-datuming: A case study. Geophysics, 63: 25-38. doi: 10.1190/1.1444319.

Zhu, T., Cheadle, S., Petrella, A. and Gray, S., 2000. First-arrival tomography: Method and application. Geophysics, 74(6): WCC1-WCC26, doi: 10.1190/1.3238367.

APPENDIX

TRAVELTIME AND AMPLITUDE

In the frequency-wavenumber domain, (ω,k_x), the wavefield recorded at a receiver can be expressed as $F(\omega)\exp(-jk_xx_g)$. Here, j is the imaginary unit, x_g is the lateral coordinate of the receiver, and $F(\omega)$ is the Fourier transform of the time series. Assuming a laterally invariant medium, we have the downward continuation of the recorded wavefield by following the phase-shift method (Gazdag, 1978) as

$$\tilde{P}(k_x,\omega,T = \sum_{i=1}^{n} \Delta T_i) = F(\omega)\exp(-jk_xx_g) \times \exp[j\omega \sum_{i=1}^{n} \Delta T_i\sqrt{\{1-(v_i^2k_x^2/\omega^2)\}}] \quad , \qquad \text{(A-1)}$$

where we divide the inhomogeneous medium into a series of vertically invariant layers: v_I is the velocity representing each layer, n is related to the depth level, and ΔT_i is the one-way vertical traveltime within each layer that reads $\Delta T_i = \Delta z_i/v_i$, with Δz_i denoting the thickness of the layer.

Defining the lower horizontal surface of the m-th layer as the datum, we have the one-way traveltime from the shot or receiver to the datum level as $T_1 = \Sigma_{i=1}^{m}\Delta T_i$ and from the datum level to the imaging point level as $T_2 = \Sigma_{i=m+1}^{n}\Delta T_i$. The time shift in the third term of the right-hand side of eq. (A-1) can be expressed by the Taylor expansion as

$$\sum_{i=1}^{n} \Delta T_i\sqrt{\{1-(v_i^2k_x^2/\omega^2)\}} = \sum_{i=1}^{n} \Delta T_i - (k_x^2/2\omega^2) \sum_{i=1}^{n} \Delta T_iv_i^2 - (k_x^4/8\omega^4) \sum_{i=1}^{n} \Delta T_iv_i^4$$

$$- \ ... + \sum_{i=m+1}^{n} \Delta T_i - (k_x^2/2\omega^2) \sum_{i=m+1}^{n} \Delta T_iv_i^2 - (k_x^4/8\omega^4) \sum_{i=m+1}^{n} \Delta T_iv_i^4 - \ ... \ . \qquad \text{(A-2)}$$

By introducing two effective velocity parameters of $V_0 = \sqrt{\{(1/T_1)\Sigma_{i=1}^{m}\Delta T_iv_i^2\}}$ and $V_{rms} = \sqrt{\{(1/T_2)\Sigma_{i=m+1}^{n}\Delta T_iv_i^2\}}$, we can approximate the time shift of eq. (A-2) as

$$\sum_{i=1}^{n} \Delta T_i\sqrt{\{1-(v_i^2k_x^2/\omega^2)\}} \approx \Delta T_1\sqrt{\{1-(V_0^2k_x^2/\omega^2)\}} + \Delta T_2\sqrt{\{1-(V_{rms}^2k_x^2/\omega^2)\}} \ . \qquad \text{(A-3)}$$

Eq. (A-3) is valid even when m is negative or zero. A negative m means that the datum is above the receiver. In this case, we have $T_1 = -\Sigma_{i=m}^{0}\Delta T_i$ and $V_0 = \bar{v}$ with $\bar{v}$ denoting the velocity of the medium that floods topography.

Substituting eq. (A-3) into (A-1) and then performing the spatial inverse Fourier transform, we have

$$P(x,\omega,T) = (\omega/2\pi)\int F(\omega)\exp\{j\omega[T_1\sqrt{(1-V_0^2p_x^2)} + T_2\sqrt{(1-V_{rms}^2p_x^2)} + p_x(x-x_g)]\}dp_x \quad , \tag{A-4}$$

where $p_x = k_x/\omega$ denotes the ray parameters in the x-direction. In eq. (A-4), we replace the integral variables k_x with p_x.

According to the method of the stationary phase (Bleistein, 1984), the main contribution of the integral in eq. (A-4) comes from point p_x in which the phase of the integrand is stationary, where

$$\partial\phi(p_x)/\partial p_x = 0 \quad , \tag{A-5}$$

and where

$$\phi(p_x) = T_1\sqrt{(1-V_0^2p_x^2)} + T_2\sqrt{(1-V_{rms}^2p_x^2)} + p_x(x-x_g) \quad . \tag{A-6}$$

Solving eq. (A-5) yields stationary point p_x^0. The integral in eq. (A-4) is approximated by following the method of the stationary phase as

$$P(x,\omega,T) = F(\omega)\sqrt{\omega}\exp(-j\pi/4)\sqrt{\{1/2\pi|\phi''(p_x^0)|\}}\exp[-j\omega\phi(p_x^0)], \tag{A-7}$$

where

$$\phi''(p_x) = -T_1V_0^2/(1-V_0^2p_x^2)\sqrt{(1-V_0^2p_x^2)} - T_2V_{rms}^2/(1-V_{rms}^2p_x^2)\sqrt{(1-V_{rms}^2p_x^2)} \quad . \tag{A-8}$$

By defining $\eta = V_{rms}p_x/\sqrt{(1-V_{rms}^2p_x^2)}$, substituting eq. (A-6) into (A-5) yields

$$[a_1a_2^2\eta/\sqrt{\{1 + (1-a_2^2)\eta^2\}}] + \eta - a_3 = 0 \quad , \tag{A-9}$$

where $a_1 = T_1/T_2$, $a_2 = V_0/V_{rms}$, $a_3 = (x-x_g)/T_2V_{rms}$, are non-dimensional parameters.

We can solve η analytically from eq. (A-9). Substituting the positive root of eq. (A-9) into eqs. (A-6) and (A-8) gives the traveltime and amplitude of the wave propagating from the receiver to the imaging point (x,T_2) as

$$\tau = [T_2/\sqrt{(1 + \eta^2)}][1 + a_1\sqrt{\{1 + (1 - a_2^2\eta^2)\}} + \eta a_3] \quad , \tag{A-10}$$

$$\begin{aligned} A = {} & \{[1 + (1 - a_2^2\eta^2)]/[T_2V_{rms}^2(1 + \eta^2)]\} \\ & \times \{a_1a_2^2 + [1 + (1 - a_2^2)\eta^2]^{3/2}\}^{-1/2} \\ & \times \{a_1a_2^2 + [1 + (1 - a_2^2)\eta^2]^{1/2}\}^{-1/2} \quad . \end{aligned} \tag{A-11}$$